JACS
JOURNAL OF THE AMERICAN CHEMICAL SOCIETY
pubs.acs.org/JACS
Article

High Quantum Yields from Perfluorinated Binolate Erbium Complexes and Their Circularly Polarized Luminescence

Joseph A. Adewuyi and Gaël Ung*

Cite This: J. Am. Chem. Soc. 2024, 146, 7097−7104
Read Online
ACCESS | Metrics & More | Article Recommendations | Supporting Information

ABSTRACT: High quantum yield and circularly polarized luminescence (CPL) brightness values are reported from Shibasaki-type erbium complexes supported by a perfluorinated Binol ligand (F_{12}Binol). The total fluorination of the ligand circumvents nonradiative quenching from C_{sp2}-H vibrations and leads to quantum yields of up to 11% and CPL brightness values of up to 317 M^{-1} cm^{-1} (a 19- and 6-fold increase, respectively, compared to $(Binol)_3ErNa_3$). These values are the highest values for any molecular erbium complex to date, making them comparable to Yb emitters. A series of fluorinated Shibasaki-type complexes are synthesized by varying the alkali metal (K, Na, Li) in the secondary coordination sphere, leading to unexpected structural differences. NMR (^{19}F, ^{7}Li) and chiroptical spectroscopy analyses provide insights into their structural geometry. With much improved quantum yields and CPL brightness values, we provide synthetic design principles toward other practical candidates for use in quantum communication technologies.

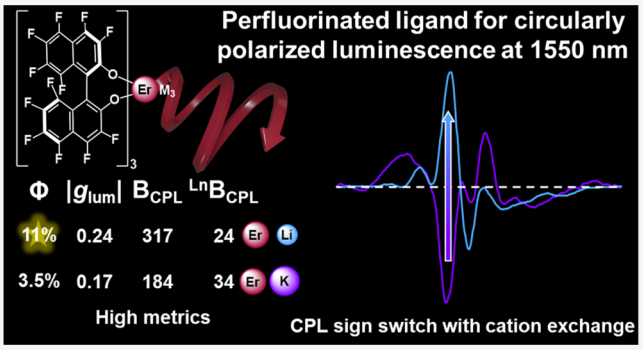

INTRODUCTION

The control of polarization of light in circularly polarized luminescence (CPL) presents the field with promising applications in quantum network[1] and quantum communication technologies.[2] To be effective for such applications, the ideal CPL emitters should emit around 1550 nm region (the telecom C-band) due to effective transmission in optical fibers within this region.[3] Therefore, lanthanide near-infrared (NIR) CPL emitters (especially erbium complexes) that maximize the dissymmetry factor (g_{lum}), quantum yield, and circularly polarized luminescence brightness (B_{CPL}) are highly desirable.

Our group has studied the chiroptical properties of several Shibasaki-type complexes emitting both in the visible and near-infrared regions.[4] Within the near-infrared region, we have reported erbium complexes of 1,1′-bi-2-naphthol (Binol) and 3,3′-diphenyl-2,2′-bi-1-naphthol (Vanol) ligands with g_{lum} values being 0.47 and 0.64 for $(Binol)_3ErNa_3$ and $(Vanol)_3ErNa_3$, respectively.[4bd] However, due to prevalent quenching in this region from C_{sp2}-H vibrations, the quantum yields (0.58% for $(Binol)_3ErNa_3$ and 0.48% for $(Vanol)_3ErNa_3$) and CPL brightness values (57.3 M^{-1} cm^{-1} for $(Binol)_3ErNa_3$ and 19.5 M^{-1} cm^{-1} for $(Vanol)_3ErNa_3$) of these complexes are low. The groups of Zinna and Di Bari have recently synthesized strong erbium CPL emitters utilizing a Shibasaki-type complex of Binol with the tetramethylguanidinium counterion $(Binol)_3Er(TMG\text{-}H)_3$,[5a] as well as pyridine-bisoxazoline complexes $Er(^{i}PrPyBox\text{-}NMe_2)_2{\cdot}3OTf$[5b] and tetrakis-heptafluorobutyrylcamphorate (hfbc) complexes $CsEr(hfbc)_4$,[5a] with g_{lum} up to 0.83, quantum yields ≤0.03%, and decent CPL brightness values ($B_{CPL} \leq 0.70$ M^{-1} cm^{-1}).[5,6] Generally speaking and irrespective of circular polarization, erbium complexes emitting in the 1550 nm region typically have low quantum yields (0.01−5%).[4−8] The luminescence of Er(III) complexes is susceptible to nonradiative vibrational quenching due to the matched energy levels of the overtones of C_{sp2}-H vibrations of the ligands and the emissive state of erbium; hence, low quantum yields are typically obtained with organic ligand-based sensitization.[9,10] Substitution of the C_{sp2}-H bonds in Binol should improve the quantum yield efficiency of the corresponding Er complexes, for example, a near-IR emitting Yb-porphyrin complex has been reported to have significantly improved and very high quantum yield (up to 63%) partly due to substitution of C−H bonds with fluorine and deuterium.[11] Seitz and co-workers reported an alternate strategy for improving the quantum yield of NIR luminescent Yb complexes by decreasing their intrinsic radiative lifetime, τ_{rad}.[12] Based on the C−H substitution approach, we hypothesized that the total fluorination of the binaphthol aromatic rings in Binol would circumvent the fluorescence quenching pathway emanating from C_{sp2}-H vibrations and thus

Received: January 24, 2024
Revised: February 9, 2024
Accepted: February 13, 2024
Published: February 27, 2024

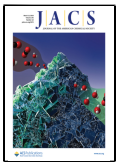

https://doi.org/10.1021/jacs.4c01165
J. Am. Chem. Soc. 2024, 146, 7097−7104

would simultaneously improve the quantum yield and CPL brightness of the erbium complex. We report here exceptionally high quantum yields (up to 11%) and CPL brightness values (up to 317 M^{-1} cm^{-1}) of Shibasaki-type Er complexes derived from the F_{12}Binol ligand. This is the first report on the coordination chemistry of F_{12}Binol. More importantly, the quantum yields of these complexes are the highest reported values beyond 1200 nm for any molecular Er(III) compound. Varying the alkali metal in the secondary coordination sphere generated structural differences in the complexes, which were investigated by NMR and chiroptical spectroscopy.

RESULTS AND DISCUSSION

Synthesis and NMR Characterization. We synthesized 2,2′-dihydroxy-3,3′,4,4′,5,5′,6,6′,7,7′,8,8′-dodecafluoro-1,1′-binaphthyl (F_{12}Binol) in a 7-step synthesis starting from readily available octafluoronaphthalene via a reported procedure by Momiyama and co-workers,[13] which is a modification of that previously reported by Piers and co-workers[14] (see the Supporting Information, Figures S1−S12 for NMR). The racemic F_{12}Binol ligand was resolved into its enantiomers using *N*-benzylcinchonidinium chloride. The enantiomerically enriched ligands were obtained in >96% *ee* before they were used for lanthanide coordination. The synthesis of the (*R*-F_{12}Binol)$_3$ErK$_3$ complex was achieved by reacting the (*R*)-F_{12}Binol ligand with $ErI_3(thf)_{3.5}$ overnight in the presence of $KN(SiMe_3)_2$ in anhydrous tetrahydrofuran at room temperature (Scheme 1). The crude complex was purified by extraction into diethyl ether after filtration of the insoluble KI byproduct. The solvent was evaporated in vacuo to obtain an off-white solid in >80% yield. The ^{19}F NMR spectrum of the complex showed six fluorine signals with integration ratios consistent with 12 F's (Figures 1 and S15) and with a single species in solution with D_3 symmetry, akin to the reported analogous [(*R*-Binol)$_3$ErNa$_3$(thf)$_6$].[4b] The fluorine signals of (*R*-F_{12}Binol)$_3$ErK$_3$ are paramagnetically shifted compared to the free ligand, indicating metal complexation (Figure 1). The enantiomer, (*S*-F_{12}Binol)$_3$ErK$_3$, was synthesized via the same protocol using (*S*)-F_{12}Binol. We note that the complexes can also be synthesized using erbium trifluoromethanesulfonate salt, Er(OTf)$_3$, but we chose the erbium iodide salt precursor due to the easier separation of the highly insoluble KI byproduct from the reaction compared to the more soluble KOTf.

Scheme 1. Synthesis of the Er Complexes[a]

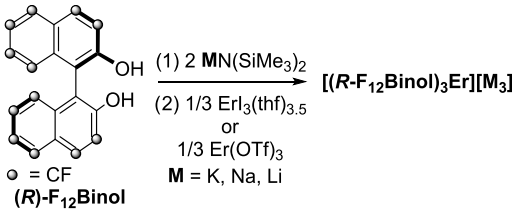

[a]The corresponding enantiomers were obtained analogously using (*S*)-F_{12}Binol.

We attempted to synthesize the Na analogues of the complex (*R*-F_{12}Binol)$_3$ErNa$_3$ using the same synthetic procedure as for the K complexes but substituting NaN(SiMe$_3$)$_2$ as a base. In the ^{19}F NMR spectrum (Figure 2b), we observed about 15 F signals suggestive of 2 species in solution: the major species (brown) having a similar structure as (*R*-F_{12}Binol)$_3$ErK$_3$ and the minor species (purple) probably having an unsymmetrical ligand geometry around the metal. Purification or separation of the complexes was unsuccessful. We attempted a different synthetic route by a salt metathesis reaction of the previously synthesized (*R*-F_{12}Binol)$_3$ErK$_3$ with sodium iodide, leveraging the insolubility of KI. From the analysis of the ^{19}F NMR spectrum (Figure 2a), the peaks of the minor species are considerably reduced though still present. A further attempt to control the speciation of (*R*-F_{12}Binol)$_3$ErNa$_3$ by performing the reaction in Scheme 1 at −78 °C led to a significant suppression of the fluorine peaks of the major species (Figure 2c) with the emergence of a new third species (black). All of the complexes synthesized from the three different synthetic routes are a mixture of at least two species in different proportions, and purification of those very soluble polyfluorinated species proved extremely challenging. Thus, the interpretation of any chiroptical results became unreliable, and we decided not to pursue those further.

We synthesized (*R*-F_{12}Binol)$_3$ErLi$_3$ by either reacting the (*R*)-F_{12}Binol ligand with $ErI_3(thf)_{3.5}$ in the presence of LiN(SiMe$_3$)$_2$ as a base (Scheme 1) or by salt metathesis cation exchange reaction of (*R*-F_{12}Binol)$_3$ErK$_3$ with lithium iodide in anhydrous tetrahydrofuran. Using both synthetic routes, the same erbium complex was obtained, whose ^{19}F NMR in deuterated acetonitrile showed 12 fluorine signals with an integration consistent with 12 inequivalent fluorine atoms (Figure 1), indicating a reduction of symmetry from D_3 to a C_3 symmetrical species in solution (see below for the Structural Discussion method). The enantiomer (*S*-F_{12}Binol)$_3$ErLi$_3$ complex was synthesized analogously starting with (*S*)-F_{12}Binol.

Optical Properties. The UV−visible absorbance spectra of (*R*/*S*-F_{12}Binol)$_3$ErK$_3$ (1.2×10^{-5} mol L^{-1}) and (*R*/*S*-F_{12}Binol)$_3$ErLi$_3$ (1.5×10^{-5} mol L^{-1}) were measured in dilute anhydrous THF solution. The absorbance spectra (250−450 nm) of both complexes showed two peaks, emanating from $\pi-\pi^*$ transition of the aromatic ring and $n-\pi^*$ transition from the lone pairs of electrons on the fluorine atoms (Figures S28 and S29). The absorbance spectra are different from that of (*R*/*S*-Binol)$_3$ErNa$_3$, which has a single absorbance peak from its $\pi-\pi^*$ transition with λ_{max} at about 360 nm.[4b] In addition, the λ_{max} of the $\pi-\pi^*$ transition in the fluorinated complexes (365 nm) is slightly (~5 nm) red-shifted compared to that in (*R*/*S*-Binol)$_3$ErNa$_3$ (360 nm), which may be due to the extended conjugation from the lone pair of the fluorine atoms. The molar extinction coefficients are 62 000 and 24 000 M^{-1} cm^{-1} (see below for molecular formula assignments) for (*R*/*S*-F_{12}Binol)$_3$ErK$_3$ and (*R*/*S*-F_{12}Binol)$_3$ErLi$_3$, respectively, which is comparable to that reported for (*R*/*S*-Binol)$_3$ErNa$_3$ at 42 000 M^{-1} cm^{-1}.[4b]

Upon excitation at 380 nm, the (*R*/*S*-F_{12}Binol)$_3$ErK$_3$ complexes in anhydrous tetrahydrofuran solution showed erbium luminescence between 1440 and 1650 nm resulting from the $^4I_{13/2} \rightarrow {}^4I_{15/2}$ transition (Figure 3, red trace). The emission pattern is different from those of previously reported Shibasaki-type complexes (Binol)$_3$ErNa$_3$ and (Vanol)$_3$ErNa$_3$ (Figure S35). The spectral width of the emission spectrum of (*R*/*S*-F_{12}Binol)$_3$ErK$_3$ is 210 nm (1440−1650 nm), which is smaller than that of (Binol)$_3$ErNa$_3$ (265 nm, from 1435 to 1700 nm). This is consistent with the F_{12}Binol ligand having a weaker ligand field strength compared to Binol as a result of perfluorination of the aromatic system. The luminescence

https://doi.org/10.1021/jacs.4c01165
J. Am. Chem. Soc. 2024, 146, 7097−7104

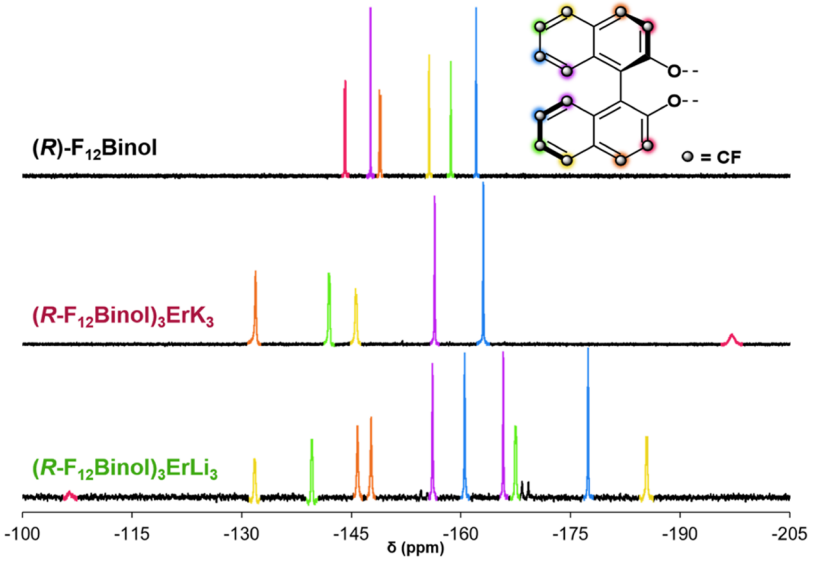

Figure 1. Comparison of the ^{19}F NMR spectrum of (*R*)-F_{12}Binol with (*R*-F_{12}Binol)$_3$ErK$_3$ and (*R*-F_{12}Binol)$_3$ErLi$_3$ showing paramagnetic shifts due to metal complexation. Assignment of the ^{19}F signals was aided by ^{19}F−^{19}F COSY (Figures S20 and S22). Assignment of the unsymmetrical top/bottom naphthol rings in (*R*-F_{12}Binol)$_3$ErLi$_3$ could not be done confidently; thus, the colors have been kept identical.

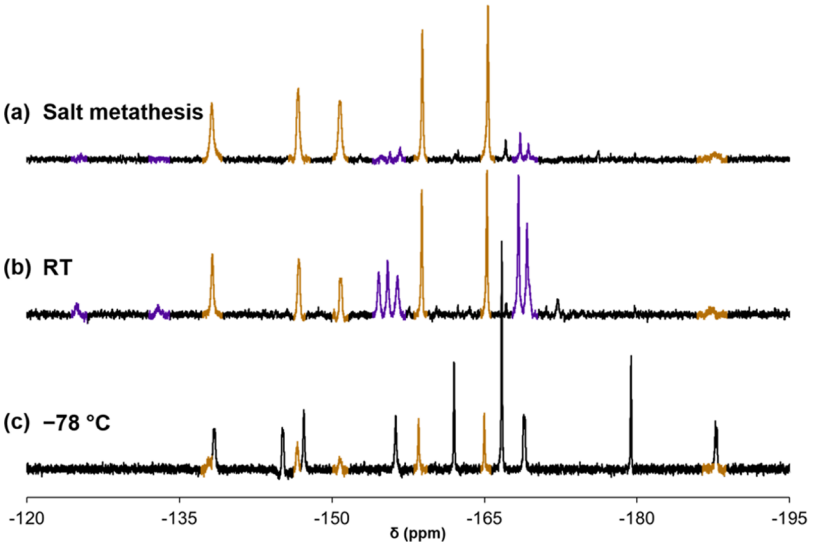

Figure 2. Comparison of the ^{19}F NMR spectra of (*R*-F_{12}Binol)$_3$ErNa$_3$ from different synthetic routes.

lifetime decay of (*R*/*S*-F_{12}Binol)$_3$ErK$_3$ was fitted to a single exponential, consistent with a single species in solution, and the half-life was measured to be 10 μs. This value is at the top end of other molecular erbium complexes (1−14 μs)[4−7] except for a fluorinated imidodiphosphinate erbium complex with a lifetime of 741 μs.[8] The quantum yield of (*R*/*S*-F_{12}Binol)$_3$ErK$_3$ was measured to be relatively high at 3.5%, which is attributed to decreased nonradiative quenching pathways. This is an order of magnitude higher than that of (Binol)$_3$ErNa$_3$ (0.58%) and on the high end of other comparable molecular erbium complexes (0.01−5%).[4−8]

The luminescence of (*R*/*S*-F_{12}Binol)$_3$ErLi$_3$ was also measured, and an erbium luminescence between 1440 and 1650 nm was observed resulting from the $^4I_{13/2} \rightarrow {}^4I_{15/2}$ transition (Figure 3, green trace). Its emission pattern is different from that of (*R*/*S*-F_{12}Binol)$_3$ErK$_3$ supporting the observation of the difference in their ^{19}F NMR spectra, thus confirming two distinct binding environments around the erbium center between the Li and K complexes. The similar width in the emission spectra of (*R*/*S*-F_{12}Binol)$_3$ErK$_3$ and (*R*/*S*-F_{12}Binol)$_3$ErLi$_3$ (1440−1650 nm) is consistent with similar crystal field strength of the ligand, but their different emission patterns suggest different ligand arrangements, leading to different crystal field splitting. The lifetime decay was fitted to a single exponential, consistent with a single species in solution, and the half-lifetime was determined to be 34 μs. The quantum yield of (*R*-F_{12}Binol)$_3$ErLi$_3$ was measured to be 11%. This is the highest reported quantum yield of a molecular erbium complex to date (19-fold increase compared to 0.58% for (Binol)$_3$ErNa$_3$) and of any emissive species emitting beyond 1200 nm. Both the lifetime and quantum yield values of (*R*/*S*-F_{12}Binol)$_3$ErLi$_3$ are approximately three times those of (*R*/*S*-F_{12}Binol)$_3$ErK$_3$.

Chiroptical Properties. The circular dichroism (CD) spectra of the erbium complexes, (*R*/*S*-F_{12}Binol)$_3$ErK$_3$ and (*R*/*S*-F_{12}Binol)$_3$ErLi$_3$, were measured from dilute tetrahydrofuran

https://doi.org/10.1021/jacs.4c01165
J. Am. Chem. Soc. 2024, 146, 7097−7104

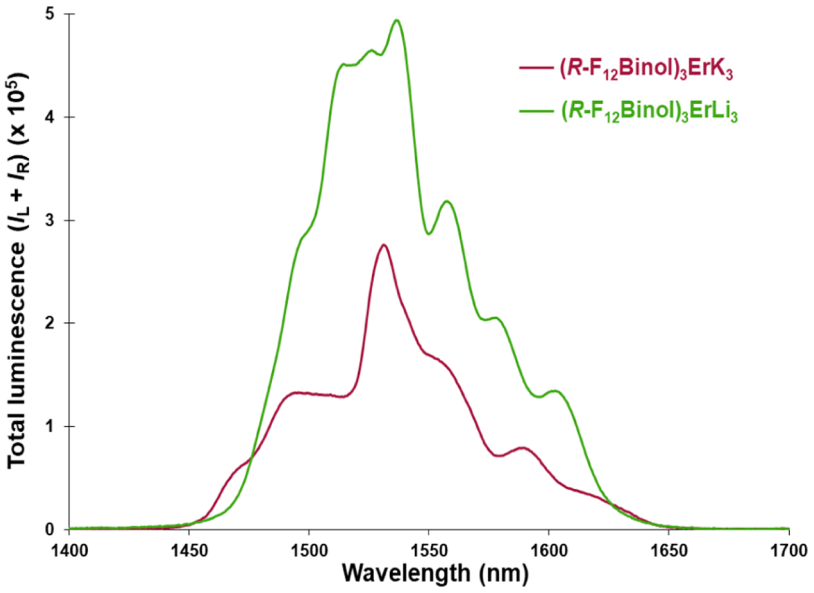

Figure 3. Comparison of the emission spectra of $(R\text{-}F_{12}Binol)_3ErK_3$ (red) and $(R\text{-}F_{12}Binol)_3ErLi_3$ (green) in tetrahydrofuran solutions (1.2×10^{-5} mol L^{-1}) at room temperature. Excitation was at 380 nm. Bandpass: 10 nm.

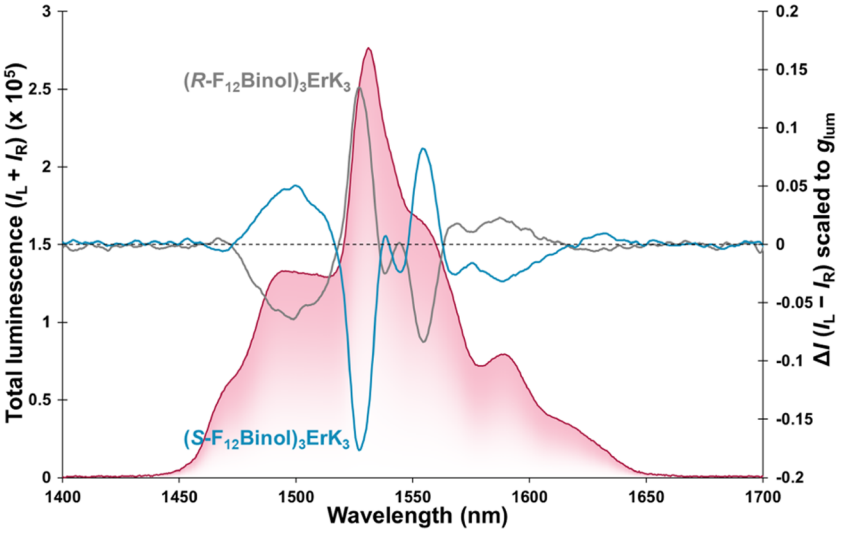

Figure 4. CPL spectra of $(R\text{-}F_{12}Binol)_3ErK_3$ (gray) and $(S\text{-}F_{12}Binol)_3ErK_3$ (blue) in tetrahydrofuran solutions (1.2×10^{-5} mol L^{-1}) at room temperature. See Figure S30 for the g_{lum} plot. Excitation at 380 nm. Bandpass: 10 nm.

solutions (1×10^{-6} mol L^{-1}). The CD spectra showed distinguishing spectral features between 250 and 400 nm for both $(R/S\text{-}F_{12}Binol)_3ErK_3$ (Figure S37) and $(R/S\text{-}F_{12}Binol)_3ErLi_3$ (Figure S38), which are different from one another and different from those of the free ligands (Figure S39). This further corroborated that the complexes likely have different coordination structures in the ground state, as previously shown by ^{19}F NMR analysis. The signs in the CD spectra remained largely positive for (R)-$F_{12}Binol$ and its corresponding Er complexes, $(R\text{-}F_{12}Binol)_3ErK_3$ and $(R\text{-}F_{12}Binol)_3ErLi_3$, while the sign is negative for the (S)-enantiomer of both the free ligand and its Er complexes (Figures S37−S39).

The circularly polarized luminescence spectrum of $(R\text{-}F_{12}Binol)_3ErK_3$ was measured from anhydrous tetrahydrofuran solution (1.2×10^{-5} mol L^{-1}) at room temperature. While for $(Binol)_3ErNa_3$ and $(Vanol)_3ErNa_3$, CPL was not detected below 1510 nm,[4] and we observed a strong CPL signal between 1470 and 1520 nm with a g_{lum} value of up to −0.12 centered at 1500 nm for $(R\text{-}F_{12}Binol)_3ErK_3$ (Figures 4 and S30). The strongest g_{lum} value of +0.17 was observed around 1526 nm, while g_{lum} values of up to −0.12 and +0.07 were obtained at 1555 and 1587 nm, respectively. The CPL spectrum of $(S\text{-}F_{12}Binol)_3ErK_3$ was an expected mirror image with dissymmetry factors of opposite sign. Although the g_{lum} values of $(R/S\text{-}F_{12}Binol)_3ErK_3$ were lower than those of $(Binol)_3ErNa_3$ ($|g_{lum}| = 0.47$) and $(Vanol)_3ErNa_3$ ($|g_{lum}| = 0.64$), when these values were combined with quantum yield and molar absorptivity, the CPL brightness[15] for $(R/S\text{-}F_{12}Binol)_3ErK_3$ was calculated to be 184 M^{-1} cm^{-1}. This CPL brightness value was 1 order of magnitude higher than that of $(Binol)_3ErNa_3$ (B_{CPL} = 57.3 M^{-1} cm^{-1}) and $(Vanol)_3ErNa_3$ (B_{CPL} = 19.5 M^{-1} cm^{-1}). The alternate $^{Ln}B_{CPL}$ (for lanthanides)[4c,6] was calculated to be 33.8 M^{-1} cm^{-1}.

The circularly polarized luminescence spectrum of $(R\text{-}F_{12}Binol)_3ErLi_3$ was also measured from dilute tetrahydrofuran

https://doi.org/10.1021/jacs.4c01165
J. Am. Chem. Soc. 2024, 146, 7097−7104

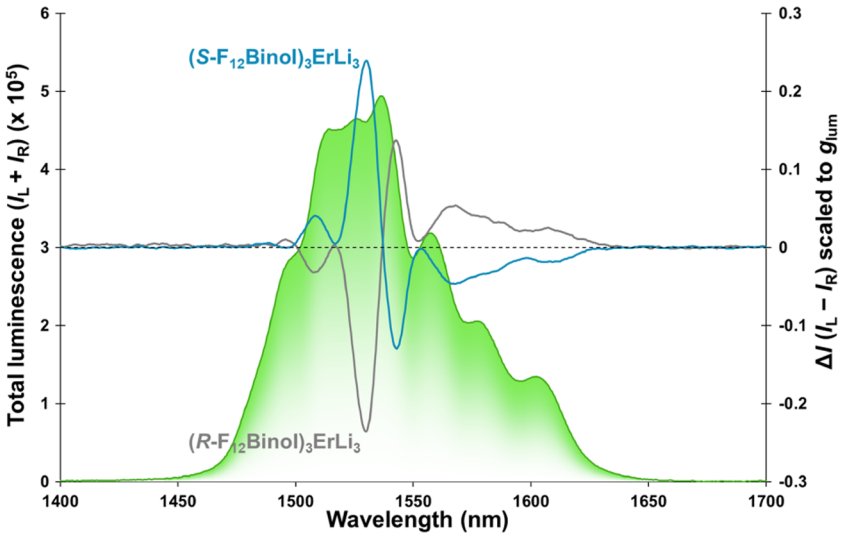

Figure 5. CPL spectra of $(R\text{-}F_{12}Binol)_3ErLi_3$ (gray) and $(S\text{-}F_{12}Binol)_3ErLi_3$ (blue) in tetrahydrofuran solutions (1.5×10^{-5} mol L^{-1}) at room temperature. See Figure S31 for the g_{lum} plot. Excitation at 380 nm. Bandpass: 10 nm.

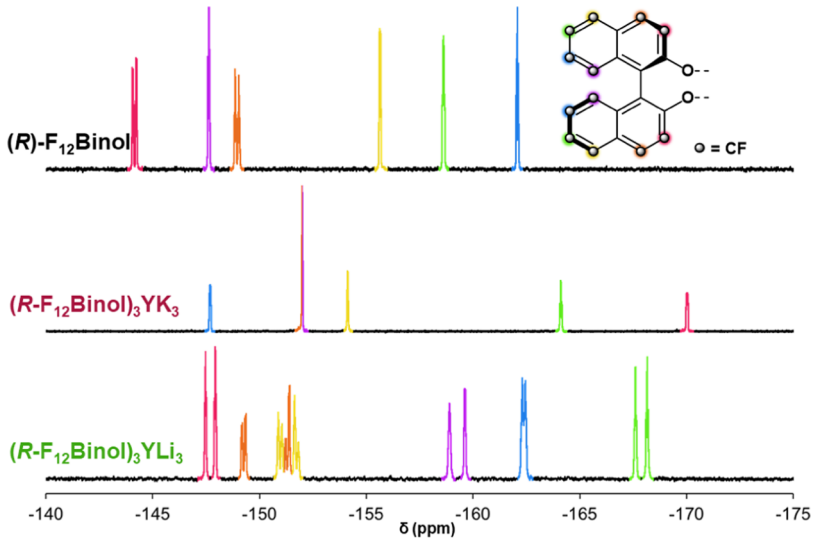

Figure 6. Comparison of the ^{19}F NMR of (R)-$F_{12}Binol$ with $(R\text{-}F_{12}Binol)_3YK_3$ and $(R\text{-}F_{12}Binol)_3YLi_3$ showing a resonance shift due to metal complexation. Assignment of the ^{19}F signals was aided by $^{19}F-^{19}F$ COSY (Figures S20 and S22). Assignment of the unsymmetrical top/bottom naphthol rings in $(R\text{-}F_{12}Binol)_3YLi_3$ could not be done confidently; thus, the colors have been kept identical.

solution (1.5×10^{-5} mol L^{-1}; Figures 5 and S31). There was minimal CPL at wavelengths less than 1500 nm. Three distinct patterns are observed in the emission spectrum between 1500 and 1550 nm, possessing g_{lum} values of −0.04, −0.24, and +0.16 at 1508, 1530, and 1544 nm, respectively. The lower energy peak at 1570 nm has a g_{lum} of +0.11 (Figure S31). The CPL spectrum of $(S\text{-}F_{12}Binol)_3ErLi_3$ was an expected mirror image with dissymmetry factors of opposite signs (Figures 5 and S31). When the CPL value is combined with the quantum yield and molar absorptivity, the CPL brightness (B_{CPL}) is calculated to be 317 M^{-1} cm^{-1}. This is the brightest erbium complex reported to date and that value is reaching those from some of the brightest ytterbium luminescent compounds: $((Binol)_3YbNa_3$ with B_{CPL} = 379 M^{-1} $cm^{-1})$[4b] and a D_4-symmetry Yb(III) helicate (B_{CPL} = 821 M^{-1} cm^{-1}).[16] The alternate $^{Ln}B_{CPL}$ (for lanthanides)[4c6] was calculated to be 23.6 M^{-1} cm^{-1}. We note that these complexes are stable in a dilute solution with very minimal decomposition (as revealed by ^{19}F NMR) even after 3 months. For comparison, at 1530 nm, which is around the telecom C-band region of interest, $(R/S\text{-}F_{12}Binol)_3ErLi_3$ has a higher $|g_{lum}|$ value of 0.24 compared to 0.17 for $(R/S\text{-}F_{12}Binol)_3ErK_3$.

Structural Discussion. Due to the significant and unexpected differences in the ^{19}F NMR and (chir)optical spectra of the $(R/S\text{-}F_{12}Binol)_3ErK_3$ and $(R/S\text{-}F_{12}Binol)_3ErLi_3$ complexes, we sought to elucidate their structures. Unfortunately, the growth of single crystals suitable for XRD analyses proved very challenging due to the extreme solubility of those perfluorinated species. Without a solid-state structure starting point, we sought structural insights based on solution techniques, combustion analyses, and literature precedents on Shibasaki-type coordination complexes. To reduce the risk of misinterpreting the NMR spectroscopy data due to paramagnetism, we synthesized the diamagnetic yttrium complexes $(R\text{-}F_{12}Binol)_3YK_3$ and $(R\text{-}F_{12}Binol)_3YLi_3$. The ^{19}F NMR spectra have similar patterns to those of the Er analogue,

https://doi.org/10.1021/jacs.4c01165
J. Am. Chem. Soc. 2024, 146, 7097−7104

Table 1. Chiroptical Properties of the Er Complexes

complex	λ_{max} (nm)	ε (M^{-1} cm^{-1}) at 380 nm	Φ	$\lvert g_{lum}\rvert$	B_{CPL} (M^{-1} cm^{-1})	$^{Ln}B_{CPL}$ (M^{-1} cm^{-1})[4c6]	lifetime (μs)
$(R/S\text{-}F_{12}Binol)_3ErK_3$	1526	62 000	0.035	0.17	184	33.8	10
$(R/S\text{-}F_{12}Binol)_3ErLi_3$	1530	24 000	0.11	0.24	317	23.6	34

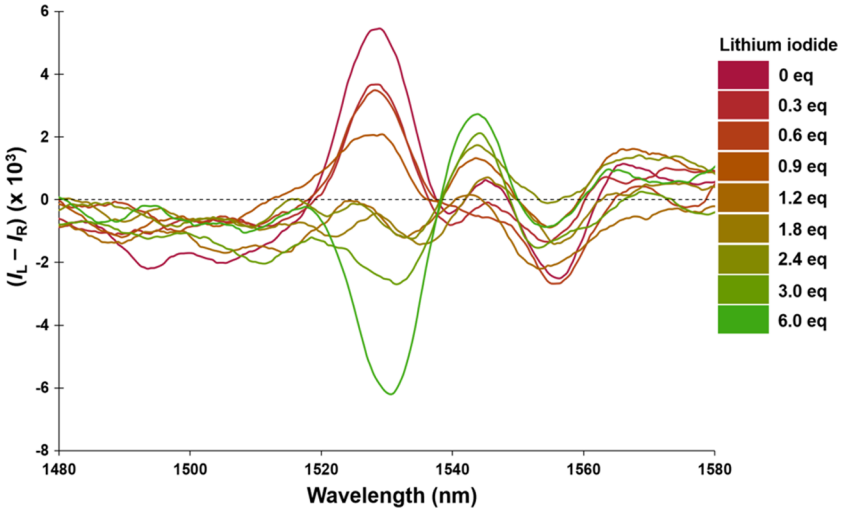

Figure 7. CPL response of $(R\text{-}F_{12}Binol)_3ErK_3$ in tetrahydrofuran solution (1.3×10^{-5} mol L^{-1}) to increasing addition of lithium iodide. Excitation at 380 nm. Bandpass: 10 nm.

with $(R\text{-}F_{12}Binol)_3YK_3$ exhibiting patterns consistent with D_3 symmetry, and $(R\text{-}F_{12}Binol)_3YLi_3$, showing patterns consistent with C_3 symmetry and unsymmetrical $F_{12}Binol$ ligands (Figures 6 and 1). Assignment of the ^{19}F signals was aided by $^{19}F-^{19}F$ COSY (Figures S20 and S22). Of interest, the signal for the fluorine "ortho" to the bound naphthol (magenta in Figures 1 and 6) has a distinct shift in both K and Li complexes, moving from the most upfield to the most downfield, respectively (also observed in the spectra of the Er analogues). The ^7Li NMR spectrum of $(R\text{-}F_{12}Binol)_3YLi_3$ showed a peak at 0.25 ppm, significantly shifting downfield from typical solvated Li^+ cations (Figure S27b). The combination of unusual ^{19}F and ^7Li chemical shifts and of an unsymmetrical $F_{12}Binol$ moiety led us to hypothesize that one of the fluorine atoms "ortho" to one bound naphthol is bound to lithium. We also note that the NMR spectra obtained from the synthesis using either $YI_3(thf)_{3.5}$ or $Y(OTf)_3$ yield identical spectra, ruling out potential anion (I or OTf) binding.

The putative Li−F bond can be supported by the strength of the lattice energy of LiF compared to KF (−1047 and −827 kJ mol^{-1}, respectively)[17] and the better matching of the size of the fluorine and lithium atoms. Such an interaction would also rigidify the $(R\text{-}F_{12}Binol)_3ErLi_3$ complex, which is consistent with the increased dissymmetry factors[18] and quantum yield observed for $(R\text{-}F_{12}Binol)_3ErLi_3$ vs $(R\text{-}F_{12}Binol)_3ErK_3$ (Table 1). We hypothesize that there is a very minimal interaction between the "ortho"-fluorine and potassium in $(R\text{-}F_{12}Binol)_3ErK_3$ and $(R\text{-}F_{12}Binol)_3YK_3$. This interaction is not strong enough to form a KF bond probably due to size mismatch between fluorine and potassium atoms, hence the preservation of the D_3 symmetry in the K complexes.

Results from the elemental analyses of $(R/S\text{-}F_{12}Binol)_3ErK_3$ are consistent with 7 bound THF molecules in the complex. This contrasts with the 6 bound THF molecules in $(R/S\text{-}Binol)_3ErNa_3$[4b] where the K cations are nestled within the complex. The elemental analyses of $(R/S\text{-}F_{12}Binol)_3ErLi_3$ are consistent with only 3 bound THF molecules in total in the structure of the complex. This is suggestive of only one bound THF molecule per Li ion, probably due to limited binding space around the Li, thus lending further support to a Li−F bond.

Additional clues about the structural differences can be extracted from the CPL emission profiles. The maximum $|\Delta I|$ observed at 1530 nm for $(R\text{-}F_{12}Binol)_3ErK_3$ is positive while that of $(R\text{-}F_{12}Binol)_3ErLi_3$ is negative (Figure S34). Such a drastic change in chiroptical properties could be explained by a change in chirality at the metal center in the resulting complex. While chirality inversion of the $F_{12}Binol$ ligands is highly unlikely as indicated by similar UV−vis CD spectra of the complexes (Figures S37 and S38), inversion of chirality at the metal has been previously observed in Shibasaki complexes, where $\Lambda\text{-}[(S\text{-}Binol)_3CeK_3]$ can be converted to $\Delta\text{-}[(S\text{-}Binol)_3CeK_3]$ in the presence of crown ether.[19] Since the CPL sign of $(R\text{-}F_{12}Binol)_3ErLi_3$ is the same as that of $\Delta\text{-}(R\text{-}Binol)_3ErNa_3$ (Figure S34), we conclude that $(R\text{-}F_{12}Binol)_3ErLi_3$ should have a Δ chirality at the metal.

To further probe the different arrangement of the $F_{12}Binol$ ligand around the erbium metal center, leading to metal-centered chirality inversion, we performed a CPL titration experiment. In order to mimic the synthesis of $(R\text{-}F_{12}Binol)_3ErLi_3$ from $(R\text{-}F_{12}Binol)_3ErK_3$ in the salt metathesis reaction described earlier, the incremental addition of lithium iodide was titrated against a solution of $(R\text{-}F_{12}Binol)_3ErK_3$ (Figure 7). This titration led to a response in both CPL and g_{lum} (Figures 7 and S36). The CPL around 1530 nm was gradually reduced with the incremental addition of lithium iodide. After about 1.2 equiv was added, the CPL has both a zero value and an inverted (negative) value. This could be attributed to a collapse of the structural coordination of $(R\text{-}F_{12}Binol)_3ErK_3$ in solution. At 3 equiv of lithium iodide addition, which should be sufficient to substitute the three K cations, the spectrum is completely inverted and similar to that

https://doi.org/10.1021/jacs.4c01165
J. Am. Chem. Soc. 2024, 146, 7097−7104

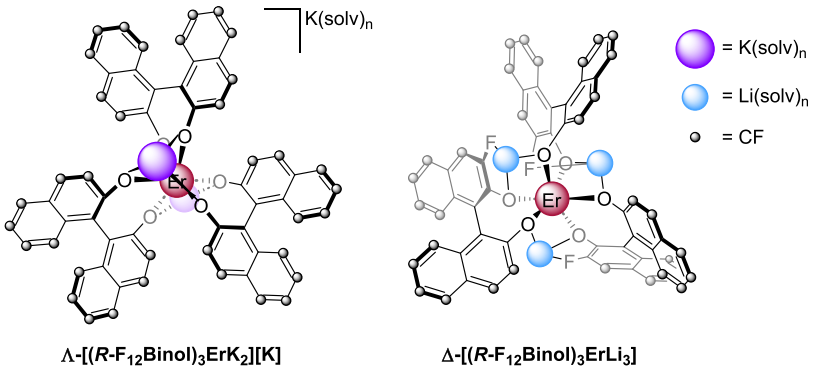

Figure 8. Proposed molecular structures of $(R\text{-}F_{12}Binol)_3ErK_3(thf)_7$ and $(R\text{-}F_{12}Binol)_3ErLi_3(thf)_3$.

of $(R\text{-}F_{12}Binol)_3ErLi_3$. Complete conversion of $(R\text{-}F_{12}Binol)_3ErK_3$ to $(R\text{-}F_{12}Binol)_3ErLi_3$, evident by a distinct inversion of the spectrum, is observed when the solution is treated with 6 equiv of lithium iodide. A similar trend is observed in the g_{lum} plot, where the g_{lum} value of +0.15 for $(R\text{-}F_{12}Binol)_3ErK_3$ is completely changed to a g_{lum} value of −0.22 when 6 equiv of lithium iodide is added (Figure S36). These values are similar to the values obtained in the CPL of the pure samples (Figures 4 and 5). We believe that the higher amount of LiI needed to fully convert these analytical samples is due to the low concentration used in our titration experiments compared to the more concentrated solutions used in the synthetic routes.

Combining NMR, elemental analyses, and CPL spectroscopies, we propose the structures shown in Figure 8, where the $(R\text{-}F_{12}Binol)_3ErK_3(thf)_7$ complex possesses Λ-chirality with the $F_{12}Binol$ coordinating through a κ^3-(O,O,O) to K, while the $(R\text{-}F_{12}Binol)_3ErLi_3(thf)_3$ complex possesses Δ-chirality with the $F_{12}Binol$ coordinating through κ^3-(F,O,O) to Li. The coordination of a lone THF molecule to lithium deduced from elemental analyses is consistent with the commonly occurring coordination number of four for lithium.

CONCLUSIONS

Using a perfluorinated Binol analogue as a ligand ($F_{12}Binol$), we report the synthesis of two chiral erbium Shibasaki-type complexes, $(R/S\text{-}F_{12}Binol)_3ErK_3(thf)_7$ and $(R/S\text{-}F_{12}Binol)_3ErLi_3(thf)_3$, with strong $|g_{lum}|$ values of up to 0.24. The K and Li complexes show drastically different chiroptical properties; a combination of NMR (^{19}F and ^{7}Li), combustion analyses, and chiroptical studies allowed us to determine their potential molecular structures. Complete fluorination of the binaphthol rings generated erbium complexes that have high quantum yields of up to 11% and CPL brightness values of up to 317 M^{-1} cm^{-1} around 1530 nm, the highest quantum yield and CPL brightness value reported to date for a molecular erbium complex. Our findings open new synthetic paths toward the design of future molecular complexes possessing even higher metrics toward potential practical applications of polarized emitters in the telecom C-band.

ASSOCIATED CONTENT

Supporting Information

The Supporting Information is available free of charge at https://pubs.acs.org/doi/10.1021/jacs.4c01165.

General information, synthetic details, NMRs, and additional chiroptical information (PDF)

AUTHOR INFORMATION

Corresponding Author

Gaël Ung − *Department of Chemistry, University of Connecticut, Storrs, Connecticut 06269, United States;* orcid.org/0000-0002-6313-3658; Email: gael.ung@uconn.edu

Author

Joseph A. Adewuyi − *Department of Chemistry, University of Connecticut, Storrs, Connecticut 06269, United States*

Complete contact information is available at: https://pubs.acs.org/10.1021/jacs.4c01165

Author Contributions

This manuscript was written through contributions of all authors. All authors have given approval to the final version of the manuscript.

Notes

The authors declare no competing financial interest.

ACKNOWLEDGMENTS

The authors acknowledge Dr. Nathan D. Schley (Vanderbilt University) for his efforts and time dedicated to screening numerous unsuccessful crystal samples. This material is based upon work supported by the National Science Foundation under grant no. CHE-2041084. They thank the College of Liberal Arts and Sciences at the University of Connecticut for partial support through its Equipment Initiative grant.

REFERENCES

(1) Simon, C. Towards a global quantum network. *Nat. Photonics* **2017**, *11* (11), 678−680.

(2) Li, X.; Voss, P. L.; Sharping, J. E.; Kumar, P. Optical-fiber source of polarization-entangled photons in the 1550 nm telecom Band. *Phys. Rev. Lett.* **2005**, *94* (5), 053601.

(3) Addanki, S.; Amiri, I. S.; Yupapin, P. Review of optical-fibers − introduction and applications in fiber lasers. *Res. Phys.* **2018**, *10* (8), 743−750.

(4) (a) Deng, M.; Schley, N. D.; Ung, G. High circularly polarized luminescence brightness from analogues of Shibasaki's lanthanide complexes. *Chem. Commun.* **2020**, *56*, 14813−14816. (b) Mukthar, N. F. M.; Schley, N. D.; Ung, G. Strong circularly polarized luminescence at 1550 nm from enantiopure molecular erbium complexes. *J. Am. Chem. Soc.* **2022**, *144*, 6148−6153. (c) Willis, B. A. N.; Schnable, D.; Schley, N. D.; Ung, G. SPINOLate lanthanide complexes for high circularly polarized luminescence metrics in the visible and near-infrared. *J. Am. Chem. Soc.* **2022**, *144*, 22421−22425. (d) Adewuyi, J. A.; Schley, N. D.; Ung, G. Vanol-supported lanthanide complexes for

strong circularly polarized luminescence at 1550 nm. *Chem. −Eur. J.* **2023**, *29*, No. e202300800.
(5) (a) Willis, O. G.; Pucci, A.; Cavalli, E.; Zinna, F.; Di Bari, L. Intense 1400−1600 nm circularly polarized luminescence from homo- and heteroleptic chiral erbium complexes. *J. Mater. Chem. C* **2023**, *11*, 5290−5296. (b) Willis, O. G.; Petri, F.; Pescitelli, G.; Pucci, A.; Cavalli, E.; Mandoli, A.; Zinna, F.; Di Bari, L. Efficient 1400−1600 nm circularly polarized luminescence from a tuned chiral erbium complex. *Angew. Chem., Int. Ed.* **2022**, *61*, No. e202208326.
(6) Willis, O. G.; Zinna, F.; Di Bari, L. NIR-circularly polarized luminescence from chiral complexes of lanthanides and d-metals. *Angew. Chem., Int. Ed.* **2023**, *62*, No. e202302358.
(7) (a) Guoa, L. J.; Zhang, J. L. Highly NIR-II luminescent erbium porphyrinoids. *J. Porphyrins Phthalocyanines* **2023**, *27*, 1348−1356. (b) Wang, T.; Wang, S.; Liu, Z.; He, Z.; Yu, P.; Zhao, M.; Zhang, H.; Lu, L.; Wang, Z.; Wang, Z.; Zhang, W.; Fan, Y.; Sun, C.; Zhao, D.; Liu, W.; Bunzil, J.-C. D.; Zhang, F. A hybrid Er(III)-bacteriochlorin near-infrared probe for multiplexed biomedical imaging. *Nat. Mater.* **2021**, *20*, 1571−1578. (c) Johnson, K. R.; Vittardi, S. B.; Gracia-Nava, M. A.; Rack, J. J.; de Bettencourt-Dias, A. Luminescent lanthanide complexes with a pyridine-bis(carboxamide)-bithiophene sensitizer showing wavelength-dependent singlet oxygen generation. *Dalton Trans.* **2020**, *49*, 6661−6667. (d) Ahmed, Z.; Mahiya, K.; Iftikhar, K. Structures and pure near-infrared photophysics of erbium and ytterbium(III) complexes incorporating fluorinated β-diketone and neutral unidentate ligands. *New J. Chem.* **2020**, *44*, 13172−13181. (e) Mara, D.; Artizzu, F.; Smet, P. F.; Kaczmarek, A. M.; Van Hecke, K.; Van Deun, R. Vibrational quenching in near-infrared emitting lanthanide complexes: A quantitative experimental study and novel insights. *Chem. −Eur. J.* **2019**, *25*, 15944−15956. (f) Nguyen, T. N.; Chow, C. Y.; Eliseeva, S. V.; Trivedi, E. R.; Kampf, J. W.; Martinic, I.; Petoud, S.; Pecoraro, V. L. One-step assembly of visible and near-infrared emitting metallacrown dimers using a bifunctional linker. *Chem. −Eur. J.* **2018**, *24*, 1031−1035. (g) Eliseeva, S. V.; Travis, J. R.; Nagy, S. G.; Smihosky, A. M.; Foley, C. M.; Kauffman, A. C.; Zaleski, C. M.; Petoud, S. Visible and near-infrared emitting heterotrimetallic lanthanide-aluminum−sodium 12-metallacrown-4 compounds: discrete monomers and dimers. *Dalton Trans.* **2022**, *51*, 5989−5996. (h) Sun, Q.; Yan, P.; Niu, W.; Chu, W.; Yao, X.; An, G.; Li, G. NIR luminescence of a series of benzoyltrifluoroacetone erbium complexes. *RSC Adv.* **2015**, *5* (81), 65856−65861. (i) Song, L.; Hu, J.; Wang, J.; Liu, X.; Zhen, Z. Novel perfluorodiphenylphosphinic acid lanthanide (Er or Er−Yb) complex with high NIR photoluminescence quantum yield. *Photochem. Photobiol. Sci.* **2008**, *7* (6), 689−693. (j) Li, Y.; Yang, H.; He, Z.; Liu, L.; Wang, W.; Li, F.; Xu, L. Significant Increment of Photoluminescence Quantum Yield by Efficiently Prohibiting Fluorescence Quenching in Erbium(III) Organic Complexes. *J. Mater. Res.* **2005**, *20* (11), 2940−2946. (k) Nah, M.-K.; Cho, H.-G.; Kwon, H.-J.; Kim, Y.-J.; Park, C.; Kim, H. K.; Kang, J.-G. Photophysical Properties of Near-Infrared-Emitting Ln(III) Complexes with 1-(9-Anthryl)-4,4,4-trifluoro-1,3-butandione (Ln) Nd and Er). *J. Phys. Chem. A* **2006**, *110* (35), 10371−10374. (l) Zhang, J.; Petoud, S. Azulene-Moiety-Based Ligand for the Efficient Sensitization of Four Near-Infrared Luminescent Lanthanide Cations: Nd3+, Er3+, Tm3+, and Yb3+. *Chem. −Eur. J.* **2008**, *14* (4), 1264−1272. (m) Ahmed, Z.; Iftikhar, K. Sensitization of Visible and NIR Emitting Lanthanide(III) Ions in Noncentrosymmetric Complexes of Hexafluoroacetylacetone and Unsubstituted Monodentate Pyrazole. *J. Phys. Chem. A* **2013**, *117* (44), 11183−11201. (n) Lama, M.; Mamula, O.; Kottas, G.; Rizzo, F.; De Cola, L.; Nakamura, A.; Kuroda, R.; Stoeckli-Evans, H. Lanthanide Class of a Trinuclear Enantiopure Helical Architecture Containing Chiral Ligands: Synthesis, Structure, and Properties. *Chem. −Eur. J.* **2007**, *13* (26), 7358−7373. (o) Hua, K. T.; Xu, J.; Quiroz, E. E.; Lopez, S.; Ingram, A. J.; Johnson, V. A.; Tisch, A. R.; de Bettencourt-Dias, A.; Straus, D. A.; Muller, G. Structural and Photophysical Properties of Visible- and Near-IR-Emitting Tris Lanthanide(III) Complexes Formed with the Enantiomers of N,N′-Bis(1-phenylethyl)-2,6-pyridinedicarboxamide. *Inorg. Chem.* **2012**, *51* (1), 647−660. (p) Shen, H.; Berezin, A. S.; Antonova, O. V.; Zvereva, V. V.; Korolkov, I. V.; Pervukhina, N. V.; Prokhorova, S. A.; Stabnikov, P. A. Crystal Structures of $[Dy(dpm)_3]_2$ and $Dy(dpm)_3$, Luminescent and X-Ray Fluorescent Study of Lanthanide(III) *Tris*-Dipivaloylmethanates. *J. Struct. Chem.* **2018**, *59* (3), 676−683.
(8) Glover, P. B.; Bassett, A. P.; Nockemann, P.; Kariuki, B. M.; Van Deun, R.; Pikramenou, C. Fully fluorinated imidodiphosphinate shells for visible- and NIR-emitting lanthanides: hitherto unexpected results of sensitizer fluorination on lanthanide emission properties. *Chem. −Eur. J.* **2007**, *13*, 6308−6320.
(9) Winkless, L.; Tan, R. H.; Zheng, Y.; Motevalli, M.; Wyatt, P. B.; Gillin, W. P. Quenching of Er(III) luminescence by ligand C-H vibrations: Implications for the use of erbium complexes in telecommunications. *Appl. Phys. Lett.* **2006**, *89*, No. 111115.
(10) Hasegawa, Y.; Wada, Y.; Yanagida, S. Strategies for the design of luminescent lanthanide (III) complexes and their photonic applications. *J. Photochem. Photobiol., C* **2004**, *5* (3), 183−202.
(11) Hu, J.-Y.; Ning, Y.; Meng, Y.-S.; Zhang, J.; Wu, Z.-Y.; Gao, S.; Zhang, J.-L. Highly near-IR emissive ytterbium(III) complexes with unprecedented quantum yields. *Chem. Sci.* **2017**, *8*, 2702−2709.
(12) (a) Doffek, C.; Seitz, M. The radiative lifetime in near-IR-luminescent ytterbium cryptates: The key to extremely high quantum yields. *Angew. Chem., Int. Ed.* **2015**, *54*, 9719−9721. (b) Kreidt, E.; Kruck, C.; Seitz, M. Nonradiative Deactivation of Lanthanoid Luminescence by Multiphonon Relaxation in Molecular Complexes. In *Handbook on the Physics and Chemistry of Rare Earths*; Elsevier, 2018; pp 30−75.
(13) Momiyama, N.; Okamoto, H.; Shimizu, M.; Terada, M. Synthetic method for 2,2′-disubstituted fluorinated binaphthyl derivatives and application as chiral source in design of chiral mono-phosphoric acid catalyst. *Chirality* **2015**, *27*, 464−475.
(14) Morrison, D. J.; Riegel, S. D.; Piers, W. E.; Parvez, M.; McDonald, R. 2,2′-disubstituted F_{12}Binapthyl derivatives: stannanes, boranes, and (R)-F_{12}Binol. *Chem. Commun.* **2006**, 2875−2877.
(15) Arrico, L.; Di Bari, L.; Zinna, F. Quantifying the overall efficiency of circularly polarized emitters. *Chem. −Eur. J.* **2021**, *27*, 2920−2934.
(16) Wang, L.; Yao, Z.; Huang, W.; Gao, T.; Yan, P.; Zhou, Y.; Li, H. Remarkable 980 nm circularly polarized luminescence from dinuclear Yb(III) helicates with a D_4 symmetry. *Inorg. Chem. Front.* **2023**, *10*, 3664−3674.
(17) Jenkins, H. D. B. Thermodynamics of the Relationship between Lattice Energy and Lattice Enthalpy. *J. Chem. Educ.* **2005**, *82*, 950−952.
(18) (a) Gendron, F.; Moore, B.; Cador, O.; Pointillart, F.; Autschbach, J.; Le Guennic, B. Ab initio study of circular dichroism and circularly polarized luminescence of spin-allowed and spin-forbidden transitions: From organic ketones to lanthanide complexes. *J. Chem. Theory Comput.* **2019**, *15* (7), 4140−4155. (b) D'Aléo, A.; Picot, A.; Beeby, A.; Williams, J. A. G.; Le Guennic, B.; Andraud, C.; Maury, O. Efficient Sensitization of Europium, Ytterbium, and Neodymium Functionalized Tris-Dipicolinate Lanthanide Complexes Through Tunable Charge-Transfer Excited States. *Inorg. Chem.* **2008**, *47*, 10258−10268. (c) Le Guennic, B.; Hieringer, W.; Görling, A.; Autschbach, J. Density functional calculations of electronic circular dichroism spectra of the transition metal complexes $[M(phen)_3]^{2+}$ (M = Fe, Ru, Os). *J. Phys. Chem. A* **2005**, *109*, 4836−4846. (d) Moore, B.; Srebro, M.; Autschbach, J. Analysis of optical activity in terms of bonds and lone pairs: The exceptionally large optical rotation of norbonenone. *J. Chem. Theory Comput.* **2012**, *8* (11), 4336−4346.
(19) Robinson, J. R.; Carroll, P. J.; Walsh, P. J.; Schelter, E. J. The impact of ligand reorganization on Cerium(III) oxidation chemistry. *Angew. Chem., Int. Ed.* **2012**, *51*, 10159−10163.

https://doi.org/10.1021/jacs.4c01165
J. Am. Chem. Soc. 2024, 146, 7097−7104